Fabrication of Barium Ferrite Films by Sol-Gel Dip Coating and Its Properties.

T. B. Byeon
Resource Utilization Team, Research Institute of Industrial Science & Technology, P.O.Box 135, 790-330, Pohang, Korea.

W. D. Cho, T. O. Kim
Dept. of Inorganic Materials, Pusan National University, Pusan 609-735, Korea.

(Received 28 February 1997)

Those were investigated, the crystallographic, morphological, and magnetic properties of barium ferrite film (SiO_2/Si substrate) prepared by sol-gel dip coating.
Appropriate sol was prepared by dissolvin barium and iron nitrate in ethylene glycol at 80 °C. To obtain the films, thermally oxidized p-type silicon substrate with (111) of crystallographic orientation were dipped into the sol, dried at 250 °C to remove organic material, and heated at 800 °C for 3 hours in air for the crystallization of barium ferrite.
It was found that the particles of barium ferrite formed on the substrate exhibited needle-like shape placing parallel to the substrate and its c-axis is long axis direction.
There was tendency that the coercive force in horizontal direction to the substrate was higher than that in vertical direction to it. This tendency was profound in large thickness.

1. Introduction

It has been interested by many workers to use ferrite films rather than bulk ferrite for microwave and millimeter-wave application because the ferrite films can provide lower cost, smaller size, and enhanced compatibility with planar circuit designs such as monolithic microwave intergrated circuits. The final goal of current research in ferrite films is combining with intergrated circuit in a system for a chip. [1] Representative materials for microwave thin films are garnets ($Y_3Fe_5O_{12}$, $(La,Y)_3(Ga,Fe)_5O_{12}$), spinels ($LiFe_5O_8$, $(Ni,Zn)Fe_2O_4$) and hexagonal ferrite ($BaFe_{12}O_{19}$).

Single-crystal films of garnet have been prepared by using technologies of liquid phase epitaxy (LPE), [2~4] chemical vapor deposition (CVD) [5] and sputter deposition [6] by many workers. Although the CVD and sputter deposition showed the possibility of its preparation, LPE is the only way with practicability for the production of the films because of its excellent quality and rapid growth rate. There have been many attempts to prepare the spinel and hexagonal ferrite films with single crystal and polycrystal by LPE [7~8] and ferrite plating method. [9] As the barium hexaferrite could be used for millimeter-wave devices in which the high magnetocrystalline anisotropy field reduce the external field required for resonance. Hexagonal ferrite film including the barium ferrite have special attention from LPE film growers.

In this study the sol's properties were investigated and barium ferrite thin films were prepared by using the sol-gel technique. Also the magnetic and crystallographic properties of the film were characterized.

2. Experimental procedure.

The films preparation process is illustrated in Fig.1.
For the preparation of sol, barium nitrate ($Ba(NO_3)_2$), iron nitrate ($Fe(NO_3)_3\ 9H_2O$), and ethylene glycol($HOCH_2CH_2OH$) was used as starting materials. The composition ratio of Fe to Ba, designated by molar ratio Fe_2/Ba, was 5.25 and the weight ratio of nitrate to ethylene glycol was 25. Ethylene glycol was heated up to 80℃ for the complete dissolution of barium and iron nitrate which has low solubility to it.

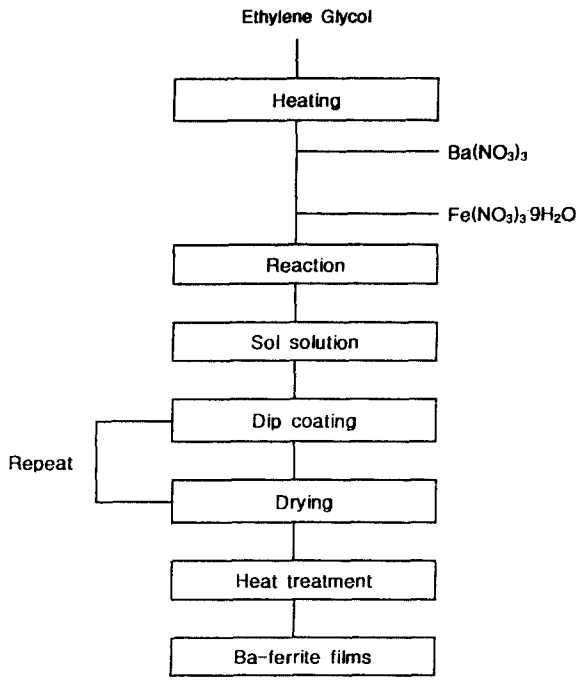

Fig. 1. Flow chart of sol-gel dip coating.

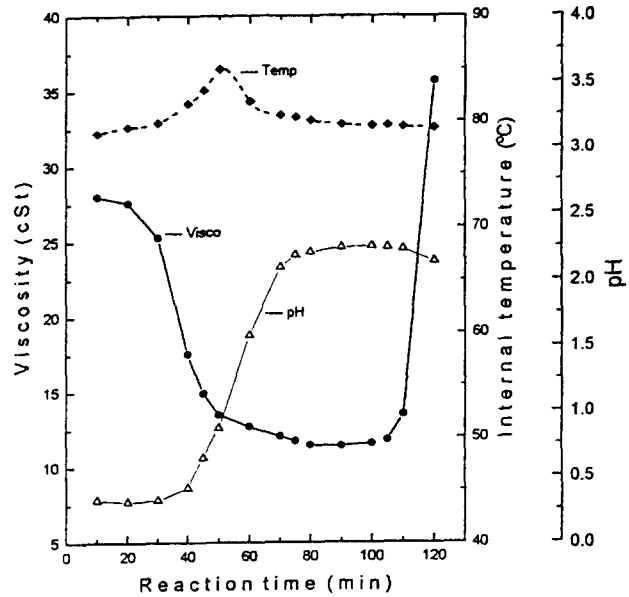

Fig. 2. Change of internal temperature, pH and viscosity of sol according to the reaction time.

Dissolution of iron nitrate into the heated ethylene glycol by stirring at 80 °C was followed by it of barium nitrate. During the whole process of sol preparation, those were measured, internal temperature, pH and viscosity. Thermally oxidized p-type silicon substrate with (111) of crystallographic orientation was dipped into the sol and drawn in the speed of 0.18mm/sec. The dipped substrates were dried at 250 °C for the removal of organic materials and heated 800 °C for 3 hours in air for the crystallization of barium ferrite layer. To obtain the desired film thickness, the dipping and drying process were repeated several times. The variation of rheological behaviors of sol with reaction and aging times were monitered by measuring its viscosity, surface tension, and pH. The crystallographic structure of thin film and gel powder were indentified by using X-ray diffraction technology using Cu K_α line as characteristic X-ray source. Also magnetic properties were characterized by using vibrating sample magnetometer a maximum applied field of 16 KOe. The film microstructure was revealed by using scanning electron microscope and transmission electron microscope. The film thickness was estimated by α-step. Depth profile of film composition was investigated by both auger electron spectroscopy and electron spectroscopy for chemical analysis.

3. Results and discussion

3.1 Properties of sol

(A) The variation of characteristics of sol.

Internal temperature, pH, and viscosity, with reaction time is shown in Fig. 2 when the external temperature is maintained at 80 °C. Internal temperature is slightly increased around 50 minutes of reaction time due to exothermic reaction and maintained constantly in other region of reaction time. Also the clearence of sol was changed from transparent to opaque around the same reaction time. These phenomena appearing around 50 minutes are presumed to be caused by rapid hydrolysis of sol. The pH of sol was increased between 50 and 70 minutes of reaction time, and maintained constantly before and after this range. The viscosity was slowly decreased until 60 minutes of reaction time, maintained constantly to 110 minutes, and then increased rapidly due to its rapid gelation.

(B) Gelation process

Based upon these results obserbed during the reaction, it is considered that the chemical structure changes of sol is proceeded into four step.

In the first step, upto 30 minutes of reaction time, while the internal temperature and pH did not be changed, the viscosity was decreased slightly. From this fact, the reaction in the first step was thought to be proceeded as follow.

$$\{[Fe(H_2O)_6](NO_3)_3\}\ 3H_2O + 12.87\ HOCH_2CH_2OH \rightarrow \{[Fe(H_2O)_6](NO_3)_3\} + 3H_2O + 12.87\ HOCH_2CH_2OH \quad (1)$$

$$\rightarrow [Fe(H_2O)_6]^{+3} + 3(NO_3)^- + 3H3O^+ + 3\ OCH_2CH_2OH^- + 9.87\ HOCH_2CH_2OH \quad (2)$$

It can be deduced from equation (1) that the viscosity is decreased due to the dissolution of water from $\{[Fe(H_2O)_6](NO_3)_3\}3H_2O$. Also the low and constant pH is caused by the formation of nitro hydroxo ion($3(NO_3)^-$), induced from

dissociation of $\{[Fe(H_2O)_6]\,(NO_3)_3\}$. It is shown in equation(2).

In the second step, from 30 to 60 minutes, the internal temperature and pH was increased slightly and rapidly respectively, while th viscosity was decreased. From these results, the reaction in the second step was considered to be proceeded as following equations.

$$Fe^{+3} + 6H_2O + 3(NO_3)^- + 3H_2O + 3H^+ + 3OCH_2CH_2OH^- + 9.87\ HOCH_2CH_2OH \quad (3)$$

$$\rightarrow Fe(OCH_2CH_2OH)_3 + 9H_2O + 3(NO_3)^- + 3H^+ + 9.87HOCH_2CH_2OH \quad (4)$$

$$\rightarrow Fe(OH)_3 + 6H_2O + 3(NO_3)^- + 3H^+ + 12.87HOCH_2CH_2OH \quad (5)$$

It is easily predicted that both increment of pH and reduction of viscosity can be caused by increment of water content due to dissociation of $[Fe(H_2O)_6]^{+3}$. Formation of ethyleneglycogate [10] , caused by reaction between Fe^{+3} and $OCH_2CH_2OH^-$, is shown in equation (4). Generally, hydrolysis is rapid in acidic region while condensation is slow in the same region. Thus the reaction, described in equation(5), is considered to be proceeded exothermically due to rapid hydrolysis. The sol prepared through the first and second steps did not wet the substrate, dipped into it.

In third step, from 60 to 105 minutes, while the viscosity was increased slightly, the changes in both internal temperature and pH were not detected. From these facts, the reaction in the third step is considered to proceeded as described in equation(6).

$$(OH)_2 - Fe - (OH) \text{ ---------- } (OH) - Fe - (OH)_2 \rightarrow (OH)_2 - Fe - O - (OH)_2 + H_2O \quad (6)$$

It is assumed from equation(6) that oligomers are formed by slow condensation and increment of viscosity, caused by polymerization of oligomers is compensated by the increment of water content, induced by condensation.

In forth step, beyond 105 minutes, both the internal temperature and pH is retained constant. However, the viscosity is increased rapidly. From these facts, the reaction in the fourth step is predicted to be proceeded as written in equation(7).

$$(OH)_2\text{-Fe-O-Fe} \begin{matrix} (OH) \cdots (OH) \\ (OH) \quad (OH) \end{matrix} \text{Fe-O-Fe-}(OH)_2 \rightarrow (OH)_2\text{-Fe-O-Fe} \begin{matrix} O \\ (OH) \quad (OH) \end{matrix} \text{Fe-O-Fe-}(OH)_2 + H_2O \quad (7)$$

It is assumed that the large polymers are formed in the result of condensation of saturated oligomers. Thus, the rapid increment of viscosity is caused by this gelation process.

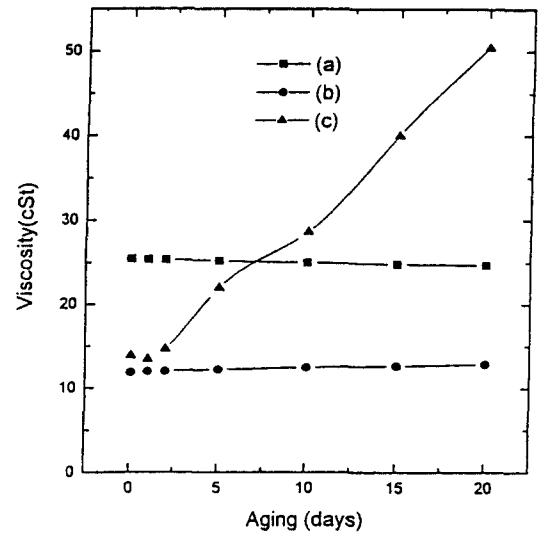

Fig. 3. Change in the viscosity of sol with aging.
(a) 30 min. (b) 90 min. (c) 110 min.

(C) The stability of sol with aging

The variation of the viscosity with aging was shown in Fig. 3. The viscosities of sol, obtained at 30 minutes and 90 minutes of reaction time, did not be changed while it, obtained at 110 minutes, was increased about four times than those. From this result, it was found that the sol, obtained over 110 minutes of it, was not suitable for coating sol.

(D) The adhesion with substrate

The surface tension, γ_{LV}, and contact angle, θ , of sol were plotted as function of the reaction time in Fig. 4. While the surface tension of sol was decreased until 60 minutes of reaction time, it was matained between 60 to 120 minutes.

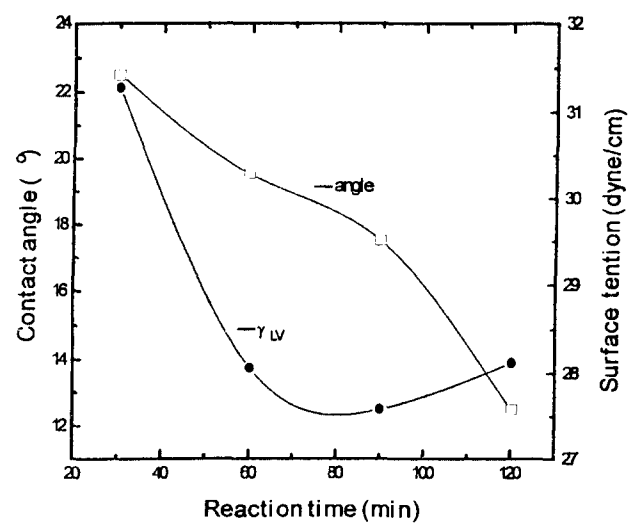

Fig.4 Change of surface tension (γ_{LV}) and contact angle according to the reaction time.

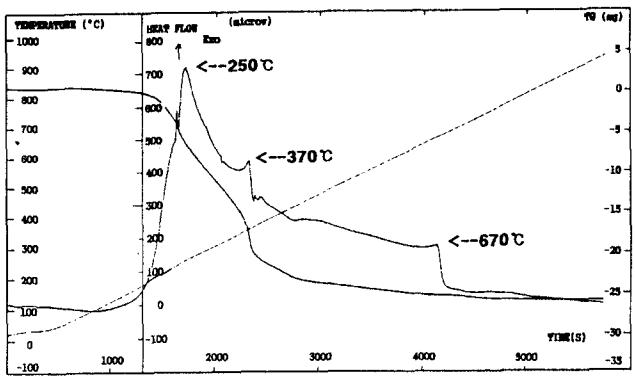

Fig. 5. TG-DTA data of dried gel powder prepared by the same method and condition as films.
(sol obtained at 90 minutes)

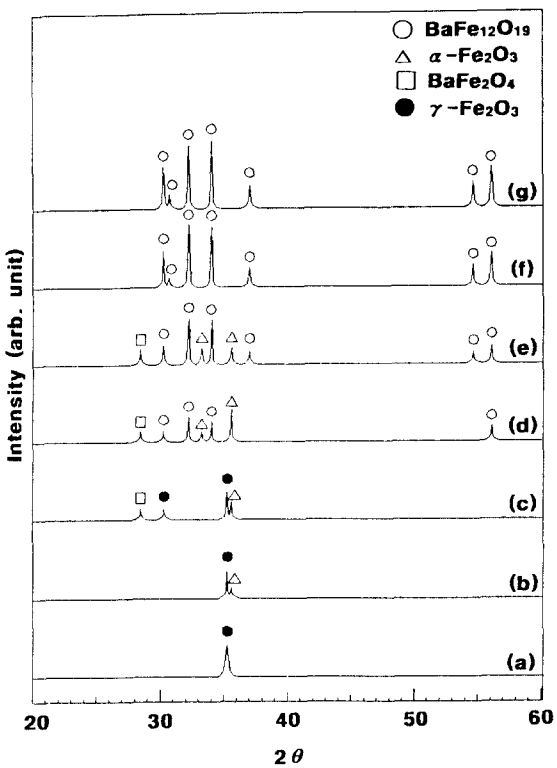

Fig.6 XRD patterns of gel powder heat-treated at various temperature.

(a) 250 °C (b) 400 °C (c) 600 °C (d) 700 °C
(e) 750 °C (f) 800 °C (g) 850 °C

The contact angle between sol and substrate was decreased as reaction time had been increased. In general, the smaller value of (1-cos θ) γ_{LV}, the more profitable sol for good coating. Thus, good coating is expected as reaction time is increased. This was verified by experiment. It was found that the sol, obtained at 90 minutes, is most suitable for the coating.

3.2 Properties of gel powder

The gel powder was prepared through the same method and condition as that used to obtain the films. TG-DTA curve of the dried gel powder is shown in Fig. 5. It was found from this curve that evaporation of organic matter was almost completed below 250 °C. Thus the drying temperature is set to 250 °C. The X-ray diffraction patterns of various gel powder, heat-treated at various temperature, is shown in Fig.6. From this patterns, it was found that γ-Fe_2O_3 was stable upto 250 °C and α-Fe_2O_3 was started to be formed from 400 °C. Barium ferrite was started to be formed at 700 °C and existed as single phase at 800 °C. Thus, the heat treatment for the crystallization of barium ferrite film was performed at 800 °C for 3 hours.

3.3 Characteristics of barium ferrite film

(A) Microstructure

Microstructures of the surface and cross-section of barium ferrite films, heat-treated at 800 °C for 3hours, were shown in Fig. 7 and Fig. 8 respectively. It was found that the microstructure consists of randomly oriented needle-like particles, whose thickness and aspect ratio were approximately 0.1μm and 5 respectively. Also the number of needle-like particles was increased with increment of the

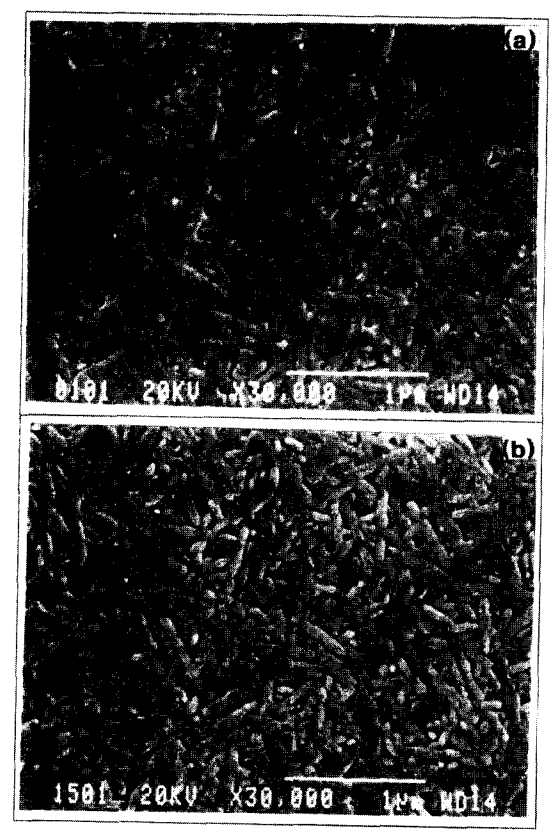

Fig.7 SEM micrographs of surface of barium ferrite thin films as a function of coating time.

(a) one time coating (b) three times coating

film thickness. Fig. 9(C) shows the bright field images of both cross-section, vertically and horizontally cut, of needle-like particle. The selected area diffraction patterns of cross-section, both vertically and horizontally cut, are shown in Fig. 9(a) and Fig. 9(b) respectively. The diffraction pattern of cross-section, vertically cut, showed six fold symmetry with zone axis of [001] direction while that, horizontally cut, showed linear shape with it of [1i0] direction. This indicates that the needle-like barium ferrite particle has its c-axis parallel to the long axis of it. It was concluded, from the observation of its microstructure and diffraction, that its easy-direction of magnetization varies from perpendicular to parallel direction to the substrate with increment of its thickness. The variation of chemical composition in barium

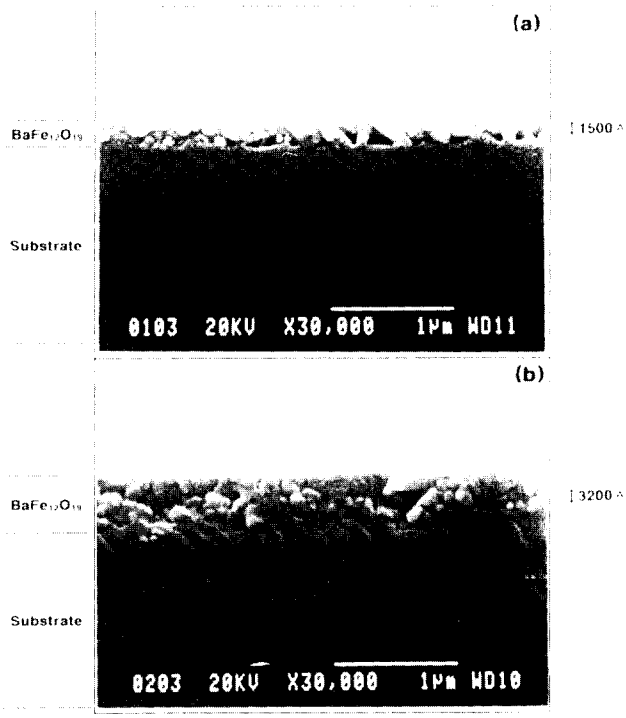

Fig.8 SEM micrographs of cross-section of barium ferrite thin films as a function of coating time.
(a) one time coating (b) three times coating

ferrite film was monitored in depth by using both AES and ESCA technique. The spectra, obtained in both technique, were shown in Fig.10 and Fig.11 As peaks of barium and iron could not be discriminated in Auger electron spectroscopy due to their overlapping, amounts of both elements did not analyzed quantitatively. However, it was confirmed from AES spectra that the film consisted of three layer, barium ferrite layer, intermediate layer of both the metal ions and silica, and silica substrate layer. It was found from ESCA spectra that the intermediate layer consisted of compound of both barium and silica. [11] Based upon the composition of the intermediate layer, it can be easily

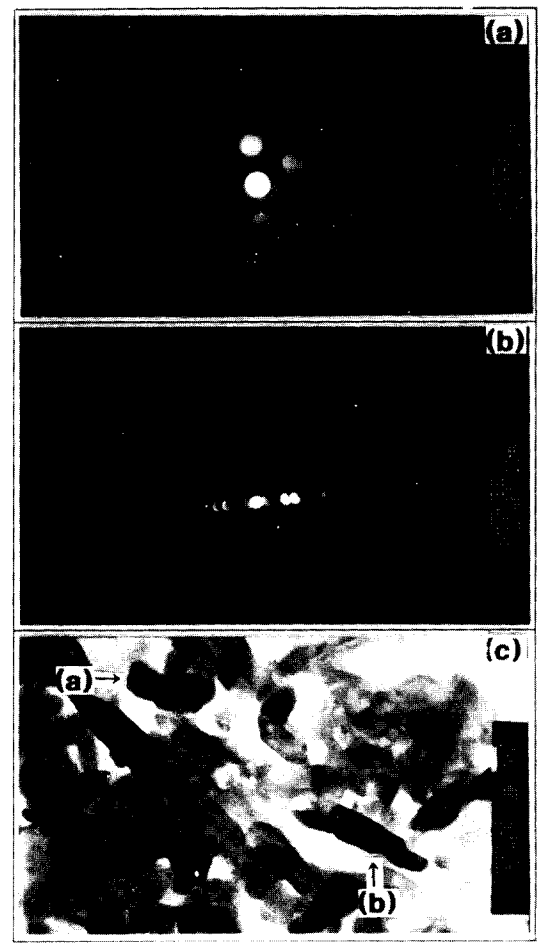

Fig.9 TEM micrographs of barium ferrite thin film prepared by one time coating.
(a) selected area diffraction pattern on the roundish grain.
(b) selected area diffraction pattern on the acicular grain.
(c) bright field image showing an acicular grain and roundish grain.

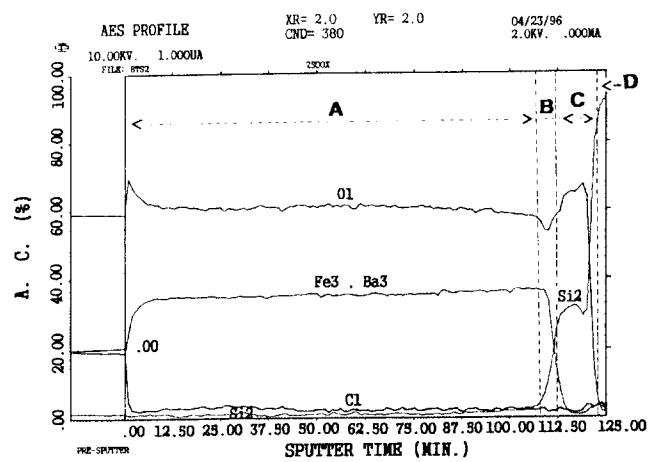

Fig.10 Depth profiles of AES spectra of barium ferrite thin film with 3000 Å thickness prepared by three times coating.
(0～107 min. : 37 Å/min. 108～125 min. : 145 Å/min.)
A : $BaFe_{12}O_{19}$ layer, B : intermediate layer
C : SiO_2 substrate layer, D : Si substrate layer

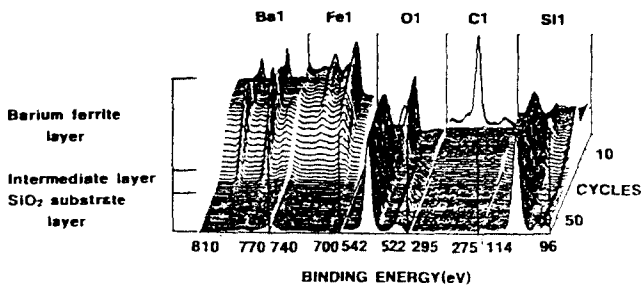

Fig.11 Depth profiles of ESCA spectra of barium ferrite thin film with 1500Å thickness prepared by one time coating. (sputter time:40Å/min., sputter time:57min.)

considered that the layer does not show magnetic property. It was also predicted that the intermediate layer acted as binding layer between the barium ferrite layer and silica substrate layer.

(B) Magnetic properties

The variation of saturation magnetization and coercive force were plotted as a function of the film thickness in Fig. 12. As the film thickness was increased, both the saturation magnetization and coercive force were enhanced. It was thought that the enhancement of saturation magnetization with the increment of film can be caused by the reduction of volume ratio of non-magnetic amorphous layer to the barium ferrite layer. In the case of the film with thickness of 150 nm, the application of magnetic field in the direction perpendicular to substrate induced the maximum value of

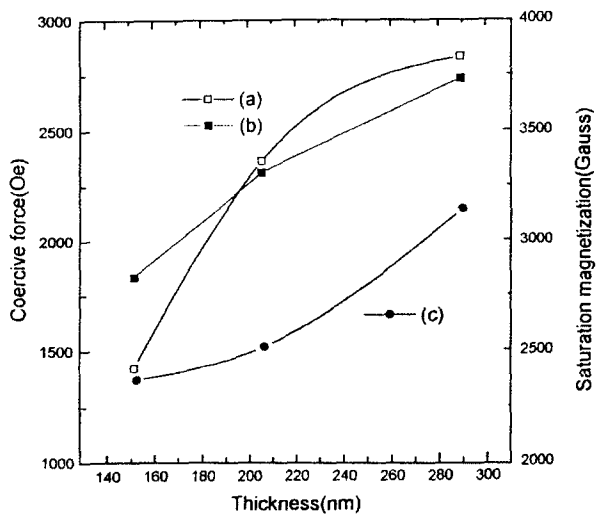

Fig. 12. Saturation magnetization and coercive force of barium ferrite thin films according to the thickness.

(a) coercive force measured with horizontal direction.

(b) coercive force measured with vertical direction.

(c) saturation magnetization.

coercive force. In other it was confirmed, based upon Stoner-Wohfarth theory [12~13], that the easy-direction of magnetization varies from perpendicular to parallel to substrate with increment in the thickness.

4. Conclusion

(1) Optimum reaction time of sol for the dip coating was 90 minutes at 80 °C.

(2) As the film thickness was increased, the needle-like particles tended to be oriented in parallel direction to the substrate.

(3) The c-axis of needle-like particle was found to be direction of long-axis.

(4) As the film thickness was increased, its coercive force, measured in the parallel direction to substrate, was higher than that, measured in the perpendicular to it.

(5) The easy-direction of magnetization varies from perpendicular to parallel to substrate with increment in the film thickness.

Reference

[1] H.L.Glass, Proc. IEEE. **76**(2), 151(1988)

[2] H.J.Levinstein, S. Licht, R.W. Landorf and S.L. Blank, Appl. Phys. Lett. **19**, 486(1971)

[3] E.A. Giess, J.D. Kuptsis and E.A.D. White, J. Cryst. Growth. **16**, 36(1972)

[4] S.L. Blank and J.W. Nielsin, J. Cryst. Growth. **17**, 302(1972)

[5] P.J. Besser, J.E. Mee, H.L. Glass and E.E.Whitcomb, Amer. Inst. Phys. Conf. Proc. **5**, 125(1971)

[6] J.J. Cuomo, V. Sadagopan, J. Deluco, P. Chaudhari and R. Rosenberg, Appl. Phys. Lett. **21**, 581(1972)

[7] P.J.M. Vander Straten and R. Metselaar, J. Cryst. Growth. **48**, 124(1981)

[8] H. Dotsch, D. Mateika, P. Roschmann and W. Tolksdorf, Mater. Res. Bull. **18**, 1209(1983)

[9] M. Abe, Y. Tamaura, Y. Goto, N. Kutamura and M. Gomi, J. Appl. Phys. **61**, 3211(1987)

[10] K. Yamaguchi, A. Kaneko, S. Kuranouchi, A. Ueno and T. Fujii, J. Mag. Soci. Japan. **12**, 343(1988)

[11] T. Tsuchiya, K. Yamachiro and J.D. Mackenzie, J. Ceram. Soci. Japan. **97**(9), 916(1989)

[12] E.C. Stoner and E.P. Wohlfarth, Natur. **160**, 650(1947)

[13] E.C. Stoner and E.P. Wohlfarth, Phil. Trans. Roy. Soc. London **A240**, 599(1948)